

**Supplementary information**

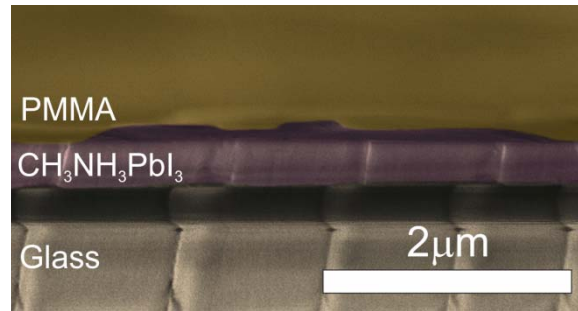
**Photophysical Analysis of the Formation of Organic-Inorganic Trihalide  
Perovskite Films: Identification and Characterization of Crystal Nucleation and  
Growth**

Miguel Anaya<sup>†</sup>, Juan F. Galisteo-López<sup>†,\*</sup>, Mauricio E. Calvo<sup>†</sup>, Cefe López<sup>‡</sup>, Hernán  
Míguez<sup>†,\*</sup>

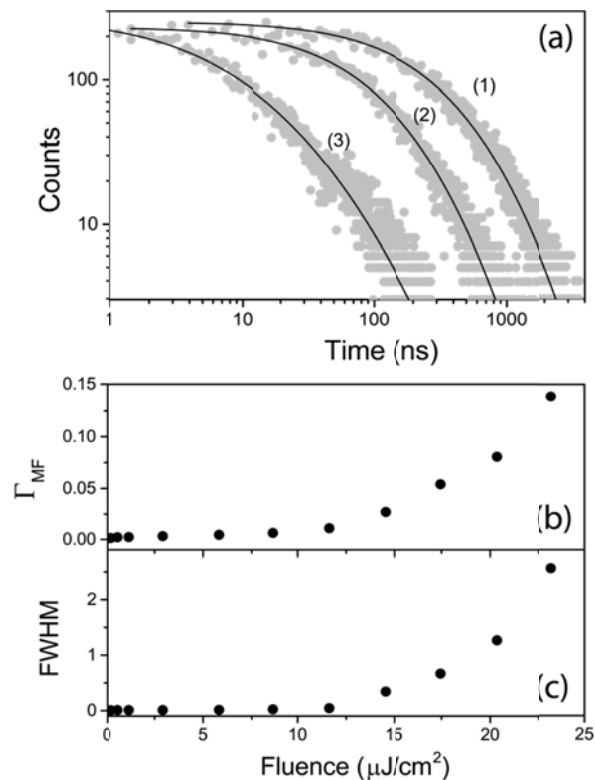
<sup>†</sup>Instituto de Ciencia de Materiales de Sevilla, Consejo Superior de Investigaciones  
Científicas (CSIC)-Universidad de Sevilla, C/Américo Vespucio 49, 41092 Sevilla,  
Spain

<sup>‡</sup>Instituto de Ciencia de Materiales de Madrid, Consejo Superior de Investigaciones  
Científicas (CSIC), C/Sor Juana Inés de la Cruz 3, 28049, Madrid, Spain

**Supplementary Figure S1:** Scanning Electron Microscopy (SEM) image showing a typical  $\text{CH}_3\text{NH}_3\text{PbI}_3$  film after annealing for 90 minutes at 100 °C. A PMMA layer was spin coated on top once the sample was cooled down to room temperature in order to prevent degradation.



**Supplementary Figure S2:** (a) Log-log plots of experimental PL decay curves (grey dots) together with fits to a log-normal distribution of decay rates (black lines) for samples pumped with 0.8 (1), 8.7 (2) and 14.5  $\mu\text{J}/\text{cm}^2$  (3). (b-c) Evolution of the most frequent value of the decay rate distribution and of its FWHM extracted from the fits as a function of pump fluence.



PL decay curves collected for a  $\lambda$  (785 nm) close to the PL maximum showing a multi-exponential behavior were fitted to a lognormal distribution of decay rates (see Supplementary Note 1). From the fits which yielded  $\chi^2$  values in the 1-1.3 range, evidencing its goodness, the most frequent value ( $\Gamma_{MF}$ ) and the full width at half maximum (FWHM) of the decay distribution were extracted. The latter can be associated with the deviation of the decay from a single-exponential behavior. Figures S1b and S1c show the evolution of  $\Gamma_{MF}$  and FWHM as the pump is increased, evidencing two regimes. In the low pump regime a nearly constant and quasi single-exponential behavior (as evidenced by a low value of the FWHM) is observed. For higher pump fluences, above  $12 \mu\text{J}/\text{cm}^2$ , the decays become faster and strongly multi-exponential corresponding to an increasing value of both  $\Gamma_{MF}$  and the FWHM (see Figures S1b-c). This transition points to a change from mono to bi-molecular recombination regimes.<sup>1,2</sup> While for the former a single-exponential behavior is expected (i.e. FWHM=0), a deviation from this behavior can occur as a consequence of sample inhomogeneity as recently pointed out by DeQuilettes and co-workers in Reference 3. In the monomolecular regime, the recombination dynamics is dominated by the filling of trap states associated with the presence of defects and thus only the concentration of a type of carrier is assumed to vary (electrons or holes depending on the nature of the defect). Upon enough pump power all trap states are filled and bimolecular recombination of electrons and holes determines the PL dynamics. While for applications in which an efficient emission is mandatory the latter regime is more suited, in order to evaluate the role of defects, whose in-situ analysis may provide relevant information on film formation, one should consider the monomolecular one.

**Supplementary Note 1:** The time evolution of the PL intensity after a pulsed optical excitation  $I(t)$  was fitted to a continuous distribution of decay rates:

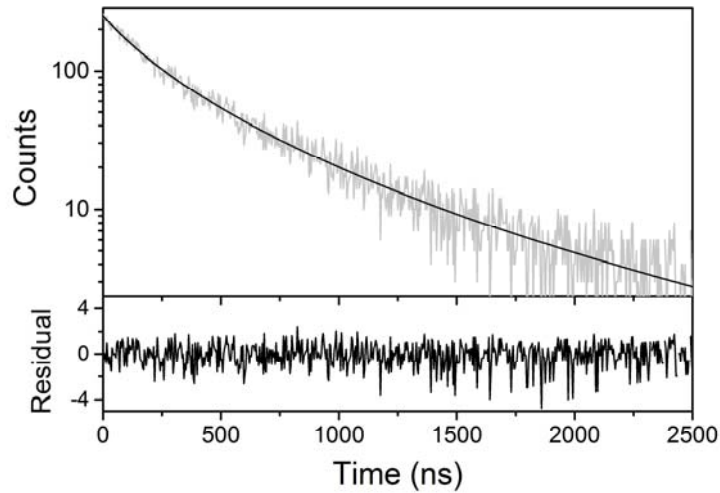
$$I(t) = \int_0^{\infty} \rho(\Gamma) e^{-\Gamma t} d\Gamma$$

where the distribution which best fitted the data is a lognormal one of the form:

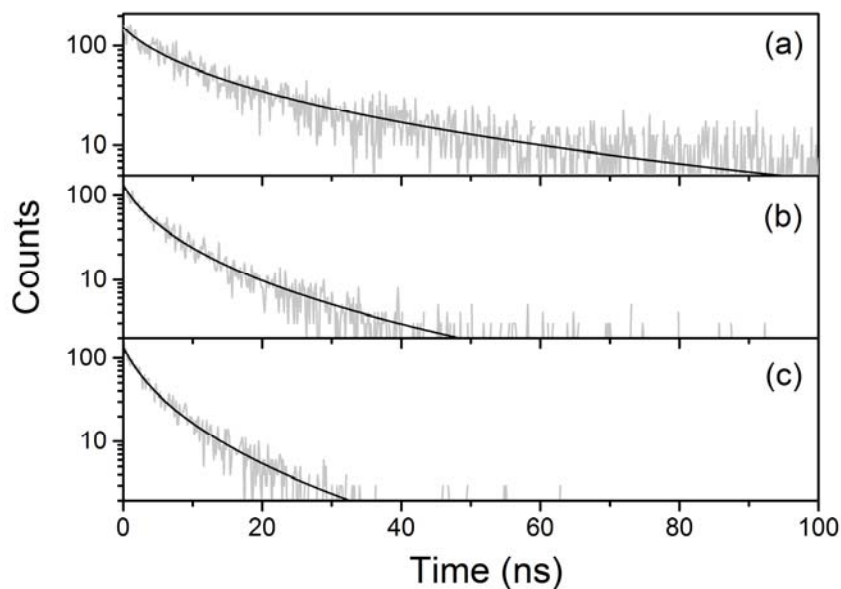
$$\rho(\Gamma) = \frac{1}{\sigma\Gamma 2\pi} e^{-\frac{1}{2}\left(\frac{\ln\Gamma - \mu}{\sigma}\right)^2}$$

being  $\Gamma$  the decay rate and  $\sigma$  and  $\mu$  the standard deviation and the mean of its logarithm.

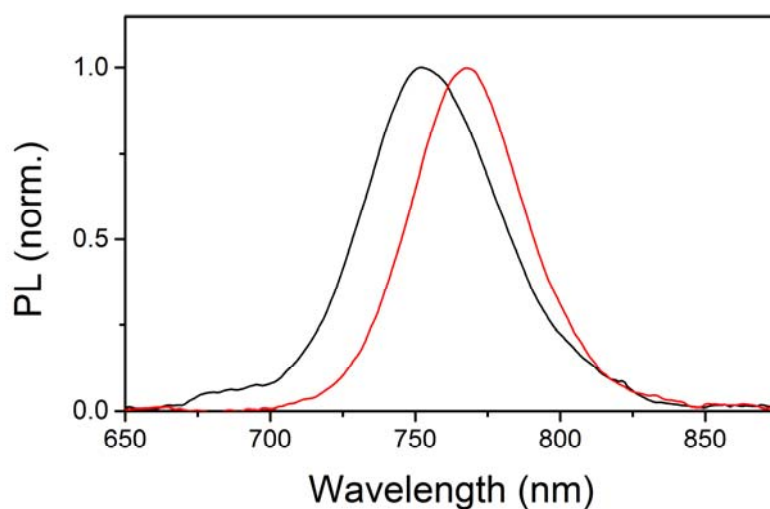
Excellent fits with  $\chi^2$  in the 1.1-1.3 range were obtained as shown in the figure below.



**Supplementary Figure S3:** Experimental PL decay curves (grey) together with fits to a distribution of decay rates for a  $\text{CH}_3\text{NH}_3\text{PbI}_3$  thin film at three different stages of the annealing process: (a) 10, (b) 20 and (c) 30 minutes.



**Supplementary Figure S4:** PL spectra of a  $\text{CH}_3\text{NH}_3\text{PbI}_3$  thin film at the end of the annealing process (90 minutes at  $100^\circ\text{C}$ ) and after cooling at room temperature for an hour are shown as black and red curves respectively.



## References:

---

- (1) Stranks, S. D.; Burlakov, V. M.; Leijtens, T.; Ball, J. M.; Goriely, A.; Snaith, H. J. Recombination Kinetics in Organic–Inorganic Perovskites: Excitons, Free Charge, and Subgap States. *Phys. Rev. Appl.* **2014**, *2*, 034007.
- (2) Yamada, Y.; Nakamura, T.; Endo, M.; Wakamiya, A.; Kanemitsu, Y. Photocarrier Recombination Dynamics in Perovskite  $\text{CH}_3\text{NH}_3\text{PbI}_3$  for Solar Cell Applications. *J. Am. Chem. Soc.* **2014**, *136*, 11610–11613.
- (3) DeQuilettes, D. W.; Vorpahl, S. M.; Stranks, S. D.; Nagaoka, H.; Eperon, G. E.; Ziffer, M. E.; Snaith, H. J.; Ginger, D. S. Impact of Microstructure on Local Carrier Lifetime in Perovskite Solar Cells. *Science* **2015**, *348*, 683-686.